CI&CEQ

Available on line at
Association of the Chemical Engineers AChE
www.ache.org.yu/CICEQ

Chemical Industry & Chemical Engineering Quarterly 14 (2) (2008) 119-136 CI&CEQ

JELENA M. JAKŠIĆ[1]
ČASLAV M. LAČNJEVAC[2]
NEDELJKO V. KRSTAJIĆ[3]
MILAN M. JAKŠIĆ[1,2]

[1]ICEHT/FORTH, Patras, Greece
[2]Faculty of Agriculture, University of Belgrade, Belgrade, Serbia
[3]Faculty of Technology and Metallurgy, University of Belgrade, Belgrade, Serbia

REVIEW PAPER

UDC 544.4+544.6:546.11+546.21:541.135.5

INTERACTIVE SUPPORTED ELECTROCATALYSTS AND SPILLOVER EFFECT IN ELECTROCATALYSIS FOR HYDROGEN AND OXYGEN ELECTRODE REACTIONS

The aim of the present paper has been to introduce the electron conductive and d-d-interactive individual and composite hypo-d-oxides of the increased altervalent capacity, or their suboxides (Magneli phases), as catalytic supports and therefrom provide: (i) The Strong Metal-Support Interaction (SMSI) effect, and (ii) the Dynamic spillover interactive transfer of primary oxides (M-OH) for further electrode reactions, and thereby advance the overall electrocatalytic activity. The d-band has been pointed out as the bonding, adsorptive and catalytic orbital. In the same context, the phenomenon and significance of the d-d-correlations both in heterogeneous catalysis and electrocatalysis are displayed and inferred. Since hypo-d-oxides feature the exchange membrane properties, the higher the altervalent capacity, the higher the spillover effect. Potentiodynamic experiments have shown that the reversible peak of the primary oxide growth on Pt, Ru and Au supported upon hypo-d-oxides and suboxides becomes distinctly increased in the charge capacity and shifts to remarkably more negative potential values, so that it starts even within the range of H-adatoms desorption, while its reduction extends until and merge with the UPD of hydrogen atoms. With wet tungstenia doped titania supported Pt catalyst in membrane cells these peaks dramatically increase in their charge capacity and reversibly become shrunk with a decreased moisture content in the feeding inert gas mixture, and vice versa. Such distinct potentiodynamic scans, in conjunction with some broaden complementary kinetic electrocatalytic improvements rising from the same hypo-d-oxide and/or suboxide interactive support effects, have been proved to be the best and comparable experimental evidence for the spillover effect of primary oxides.

Key words: catalytic spillover; electrocatalytic d-band; primary oxide (M--OH); surface oxide (M=O); SMSI (Strong Metal-Support d-d-Interaction); hypo-hyper-d-d-interactive bonding; intermetallic phases, altervalent capacity.

The present paper aim has been to reveal and establish the d-d-interelectronic correlations in the heterogeneous catalysis and electrocatalysis, and to show that the d-band is cohesive, adsorptive and (electro) catalytic orbital. Characteristic volcano curves along the transition series, which reflect the periodicity properties of elements, have then been invoked in the search for the synergism in the electrocatalytic activity. In other words, hypo-hyper-d-d-interelectronic combinations of stable intermetallic phases assembled from the ascending or hypo-d-metals and descending or hyper-d-elements, with the optimal average d-electronic configuration were best predicted and proved synergistic composites in electrocatalysis for hydrogen and oxygen electrode reactions. The further complementary aim was to show that the so-called Strong Metal-Support Interactions (SMSI) [1-4] of electrocatalysts and hypo-d-oxide catalytic supports, as based on the same d-d-interelectronic bonding effect, further contribute to increase the overall catalytic activity. Besides the orbital interactive effect, resulting in the strained interacting orbitals and thereby weakening the adsorptive bond of intermediates, the accompanying dynamic catalytic contribution from the spillover or effusion of the primary oxide (M-OH) arises at the same time. The specific

Corresponding author: Milan M. Jakšić, ICEHT/FORTH, Patras, Greece.
E-mail: milanjaksic@sezampro.yu
Phone: +381-11-3554527
Paper received: April 24, 2008.
Paper accepted: April 29, 2008.

physical and electrocatalytic properties of the latter should be more enlightened and revealed in particular for the cathodic oxygen reduction.

HYPO-HYPER-d-d-INTERELECTRONIC CORRELATIONS AND ELECTROCATALYSIS FOR THE HER

The majority of physical and chemical features of transition metals, associated with mass, electronic configuration and interactions based on the latter, obey a typical symmetric type of volcano curves along the Periodic Table, with maximum at d^5-electrons, and in this way reflect the fundamental periodicity features [5]. Therefore, when one plot cohesive *versus* surface free energy, or their volcano curves one into another, a well defined straight line dependence follows, which shows that d-band represents both the bonding and adsorptive orbital, while s,p-orbitals contribute a constant term all along the transition series [5]. In such a state of physical facts, every combination of a hypo-d-metal with any semi-series of hyper--d-elements, and *vice versa*, results in a new volcano plot and usually rather stable to extra-stable intermetallic phases [6-9]. Thus, as a consequence, all paired hypo-hyper-d-interelectronic combinations, in general, behave as the part of the Periodic Table between their individual participating periods of initial ingredients, while the other missing elements in between are replaced by the intermetallic phases of the same average d-electronic structure, and further conesquently, their electrocatalytic activity, cohesive, adsorptive and surface energies follow the same shape of almost coinciding volcano plots [10-15].

Symmetric volcano plots for cohesive (Figs. 1 and 2) [16] and surface free (Fig. 3) [17] energies feature their maximum at d^5-electrons when d-band affords a maximal number of the free d-bonding electrons [5], since paired d-electrons of the anti-bonding d-orbital do not participate in the individual transition metals cohesive interaction. Meanwhile, these paired d-electrons strongly participate in the hypo-hyper-d--d-interelectronic combinations and consequently, substantially contribute both to the intermetallic bonding effectiveness and the strained d-orbitals, with all therefrom resulting consequences, and influences the adsorption of the reacting adsorptive intermediates, and thereby on the catalytic properties of such composite electrocatalysts [10-15]. Volcano plots for the catalytic activity (*log* j_o, the logarithm of the exchange current density) in the hydrogen evolution reaction (HER) along the Periodic Table reveal the

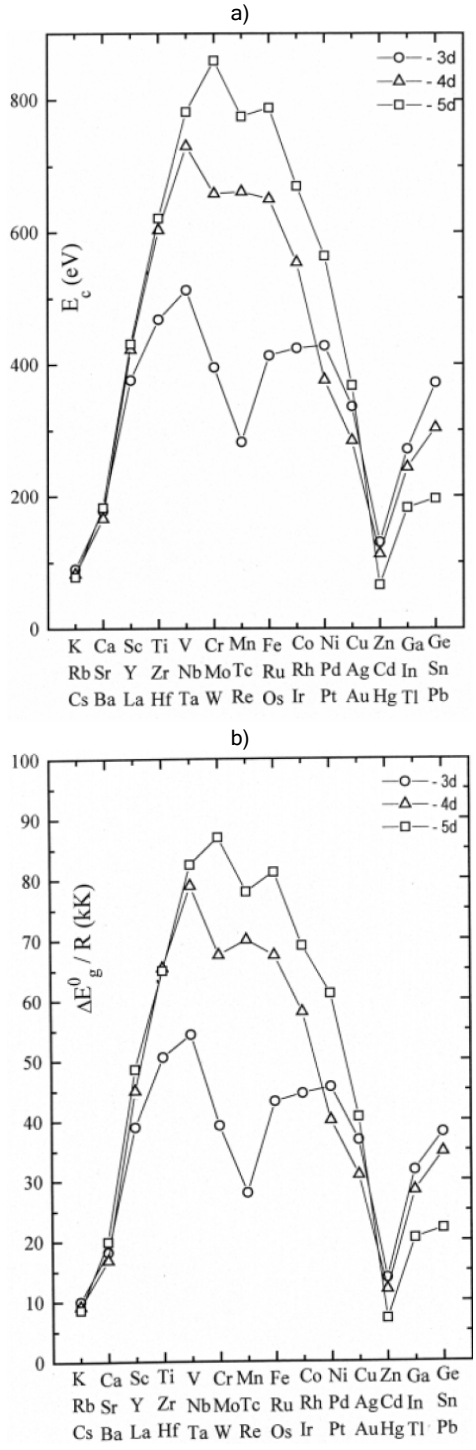

Fig. 1. a) Cohesive energy (E_c) of transition metals plotted along the Periodic Table: ○ - 3d, △ - 4d, □ - 5d level (M. M. Jakšić plots of C. Kittel values [16]); b) . Individual plot of the energy of vaporization of liquid transition metals ($\Delta E_g^o/R$) along the Periodic Table for ground atomic states at their melting points (M. M. Jakšić plot of L. Brewer values).

periodicity features of transition series, but arise asymmetric, since the optimal individual d-electronic configuration implies two empty 'seats' within the

d-band or the d^8-electronic configuration at the maximum of the electrocatalytic properties (Ni, Pd, Pt), for two H-adatoms to react by evolving as molecular species (Fig. 4) [18,19]. Since the cohesive and electrocatalytic volcano plots for the activity in the HER do not mutually overlap nor coincide, their interrelating correlations are missing for the individual elements, or need some additional corrective and correlating linear terms to bring them in a common relation, but such a straightforward relationships exist almost without exception for the hypo-hyper-d-d-interelectronic combinations (Fig. 5) [10-15]. The main conclusion therein has been that the d-orbital is the bonding, adsorptive and electrocatalytic band, and consequently, the synergism both in the HER and cathodic oxygen reduction (ORR) can only be sought within the hypo-hyper-d-d-interelectronic combinations of interatomic or interionic composites of transition elements [10-15].

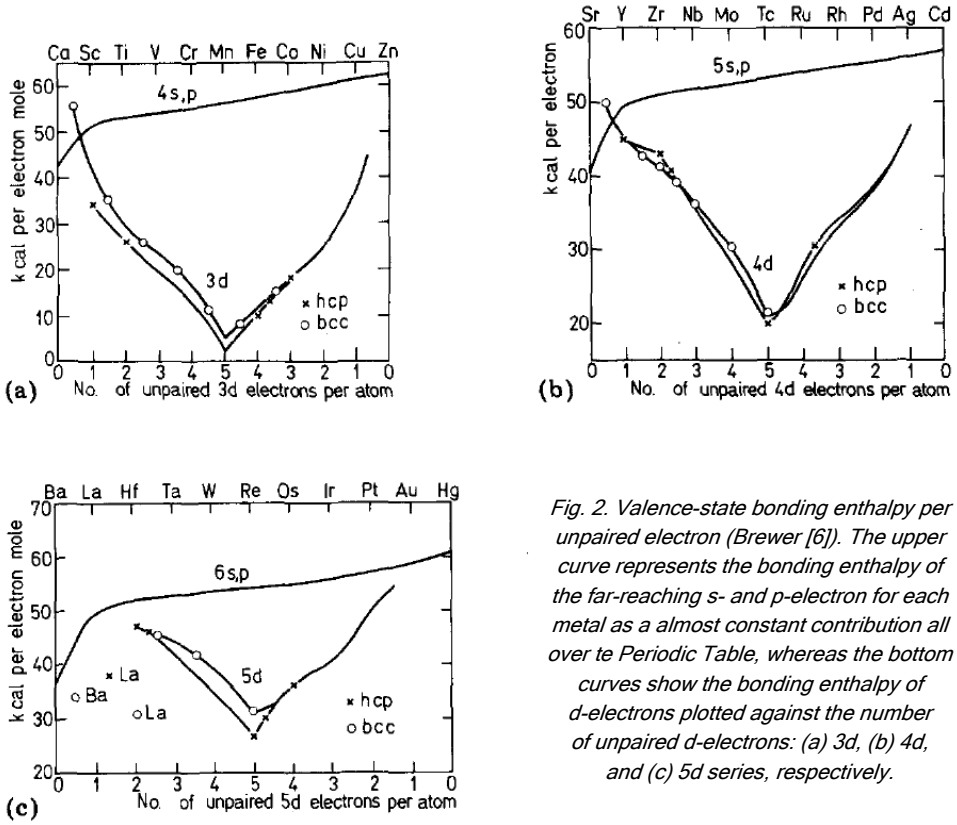

Fig. 2. Valence-state bonding enthalpy per unpaired electron (Brewer [6]). The upper curve represents the bonding enthalpy of the far-reaching s- and p-electron for each metal as a almost constant contribution all over te Periodic Table, whereas the bottom curves show the bonding enthalpy of d-electrons plotted against the number of unpaired d-electrons: (a) 3d, (b) 4d, and (c) 5d series, respectively.

Such a mutual behavior of fundamental theoretical and practical significance has therefore been used as a substantial basis for search and development of the composite synergistically active nanostructured electrocatalysts primarily for the hydrogen (HER), and recently oxygen reduction (ORR) reactions. In other words, the straightforward linear relations between the cohesive energy of bonding (or, consequently so, the surface free enthalpy [20]), adsorptive strength and electrocatalytic activity (Fig. 5), *a priori* predict the strongest of d-d-interelectronic bonding intermetallic phases, for the composite synergistically active electrocatalysts. This corresponds to the initial fact, that the stronger the interatomic bonding, the higher the d-electronic density of states. Since the optimal d-electronic configuration for the maximal electrocatalytic activity in the HER is well known (d^8) (Fig. 4), and since there exists a well defined Brewer [6-9] correlation between the crystal structure and the average d-electronic configuration, such synergistic hypo-hyper-d-d-interelectronic compositions of intermetallic phases follow straight from their phase diagrams. The coincidence between optimal peaks both of the hypo-hyper-d-d-interelectronic bonding effectiveness (Brewer intermetallic bonding correlations) [6-9] and the electrocatalytic activity for the HER confirm such interdependences [10-15]. In such a context, the application of such optimal hypo--hyper-d-interelectronic composite electrocatalysts of transition metal intermetallic phases ($MoPt_3$, $ZrNi_3$, $HfPd_3$, WPt_3, $LaNi_5$, etc.), with prevailing hyper-d-metal component, both in the intermetallic bonding effectiveness and catalytic activity, in particular when the interactive d-d-bonding supported upon suitable

electronic conductive hypo-d-oxide and/or suboxide supports with the aim to strengthen the overall d-d--correlative effect (Magneli phases [21], $Ti_nO_{(2n-1)}$, or anatase titania, TiO_2, zirconia, ZrO_2, hafnia, HfO_2, tungstenia, WO_3, and their composites), has been a broad area of further versatile synergistic advances in the electrocatalytic activity, as an additional hypo-hyper-d-d-interactive interelectronic (interatomic and/or interionic, or their combined effect) contribution, and of at least partial noble metal replacement [10-15]. In such a respect two distinct features of the so called SMSI (Strong Metal-Support Interaction) have been employed [1-4]: (i) the stronger the intermetallic hypo-hyper-d-interelectronic interaction, the less strong arises the intermediary adsorptive bond (M-H) in the RDS (rate determining step), and consequently, the more facilitated arises the intermediate reaction that leads to the increased catalytic activity (Sabatier principle in heterogeneous catalysis [22,23]) and (ii) the interactive support effect results both in the additional SMSI and a dynamic catalytic contribution of the spillover of primary oxide (M-OH) dipole (Scheme I) on the overall electrocatalytic activity [12-14].

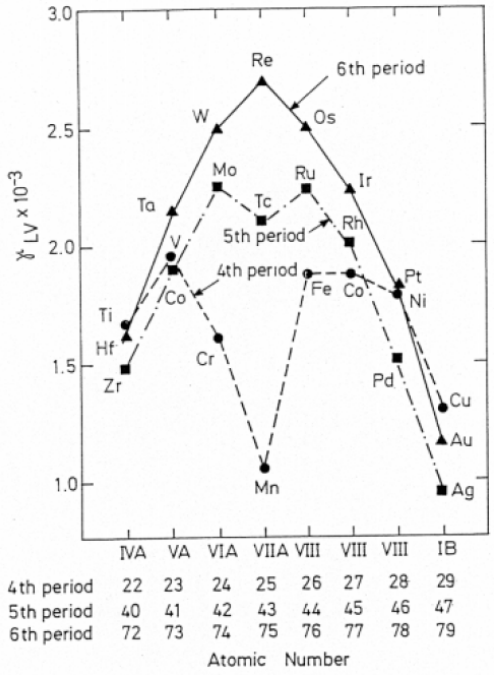

Fig. 3. Surface tension of some liquid metals (γ_{LV} - liquid surface tension, dyn cm^{-1}) at their melting points versus atomic number along transition series (after B. C. Allen [17]).

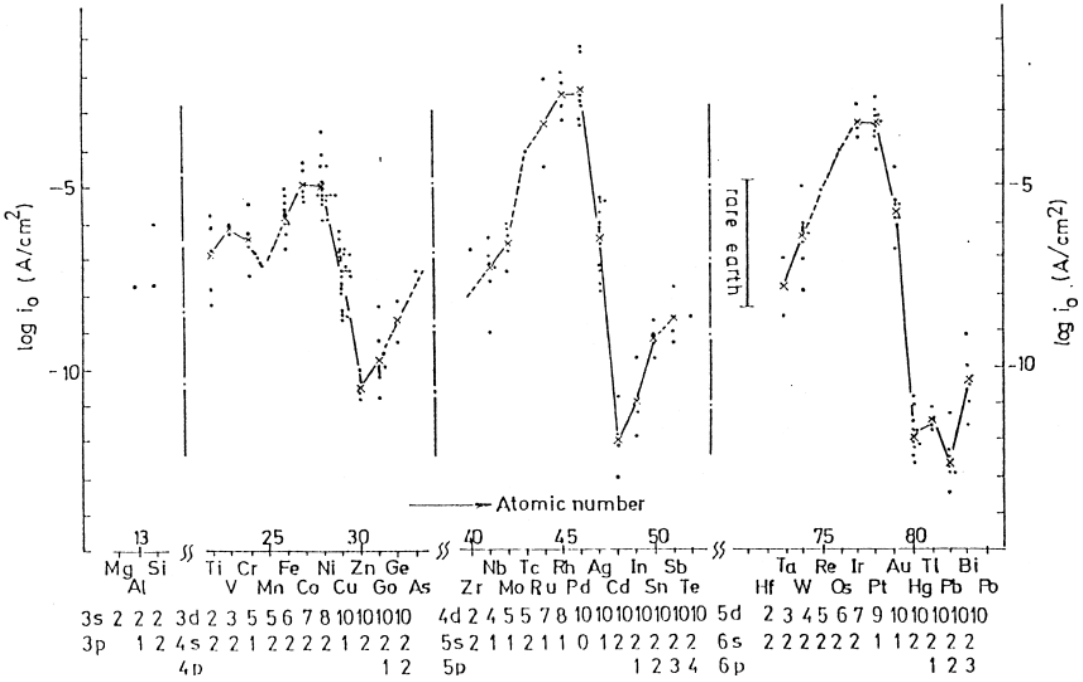

Fig. 4. Values of logarithm of exchange current density (log j_o, A cm^{-2}) for the HER on various metals plotted along the transition series in acidic media (after Kita [18]).

In fact, a bridge between heterogeneous catalysis and electrocatalysis has been established when titanium suboxides ($Ti_nO_{(2n-1)}$, in average Ti_4O_7), or Magneli phases [21] have been introduced as a rather stable and interactive catalytic support with a pronounced metallic type or electronic conductivity (300-1000 S cm^{-1}) [13,14]. Even more so, the remarkable step ahead was imposed when it has been shown that monolayers of anatase titania, zirconia, hafnia, tungstenia and their proper mixtures, under

specific conditions, in contact with metallic or even oxide type catalyst, feature the same electronic conductivity (no charge separation in XPS analysis) and much larger available surface area, with even more pronounced interactive support properties [12-14].

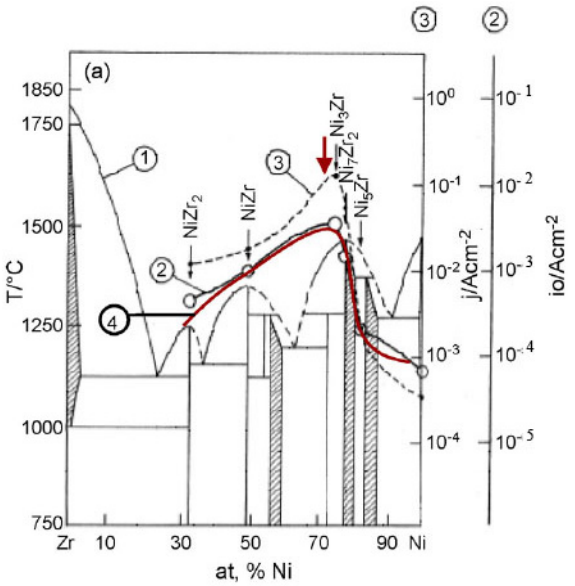

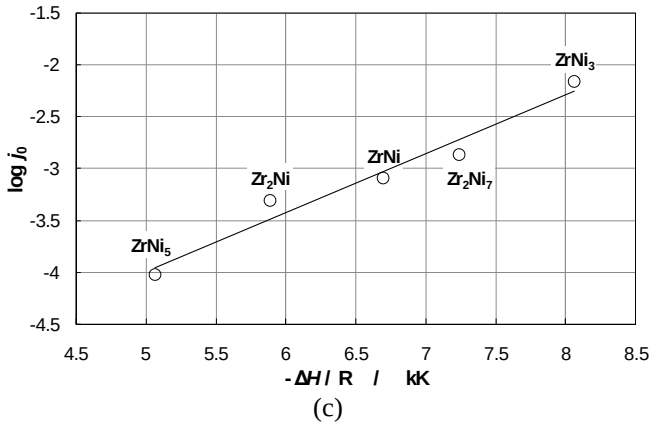

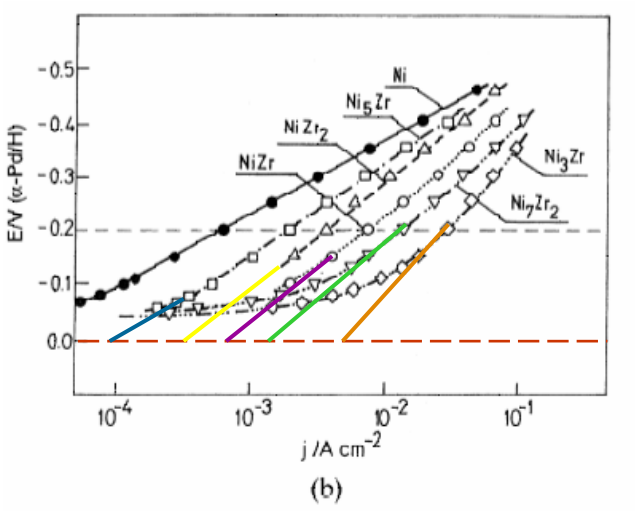

Fig. 5. Electrocatalytic activities of various intermetallic phases (polished below 1.8 in the roughness factor) along Zr - Ni phase diagram (curve 1) for the HER, taken as the exchanged current (j_o, close circles, curve 3) and relative current density changes (j, closed circuits, curve 2) at constant overvoltage (- 0.2 V), and plotted together with the cohesive energy of intermetallic phases (curve 4, arbitrary units). (Fig. 3a: Tafel plots for the HER with indicated extrapolations, 3b: Electrocatalytic activities along the Zr-Ni phase diagram, and 3c: The interplot between free enthalpy of bonding and catalytic activity (log i_o).

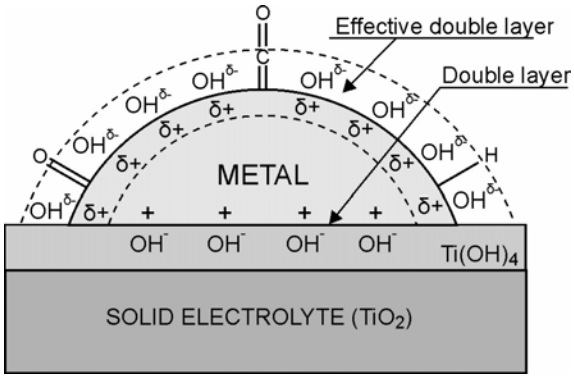

*Scheme I. Model presentation for the interactive SMSI effect resulting in the spillover transfer of the primary oxide (M-OH) as a dipole from hypo-*d*-oxide upon metallic (Pt) part of such a composite electrocatalyst (courtesy by Dr. Dimitris Tsiplakides).*

Such a hypo-hyper-d-d-interelectronic electrocatalytic behavior is the consequence of the fact that every hypo-d-electronic element belongs to the ascending and the hyper-d-metal to the descending part of the general type volcano plots (symmetric and/or asymmetric) along the transition series (Figs. 3-5), while their stable intermetallic phases replace the missing elements in-between. In such a respect, volcanic plots of the electrocatalytic activity for hydrogen electrode reactions and cohesive bonding (or surface free) energy of hypo-hyper-d-type intermetallic phases are almost overlapping and appear coincidently similar in the shape (exampled by the Zr-Ni interphase system, Fig. 5), so that the plot of one into another results in the straight line (one-to-one linear dependence), with the slope, that correlates with the constant in the Langmuir adsorption isotherm for H-ad-

atoms (Fig. 5c). Since the Brewer intermetallic bonding theory [6-9] has correlated the crystal structure with the individual and/or the average d-electronic configuration of hypo-hyper-d-d-interelectronic combinations of transition elements along multiphase and multicomponent diagrams, there exists a straightforward way to estimate the optimal d-d-synergistic composition of the intermetallic +phase to be situated at the top (peak) of such electrocatalytic volcano plots [10-15].

MEMBRANE PROPERTIES OF d-OXIDE CATALYTIC SUPPORTS AND THE PRIMARY OXIDE SPILLOVER EFFECT

The point is that the reversible peaks of primary oxides (M-OH) usually appear imprinted on cyclic voltammograms of Pt, Au, Ag, Ni, Co and many other metals at fixed potential (Fig. 6), and immediately merge into much broader irreversible peaks of the stable surface oxide (M=O) growth. Primary oxides play a decisive catalytic role both in anodic methanol and CO oxidation (CO tolerance), and cathodic oxygen reduction (ORR) [13,14]. Hypo-d-electronic oxides, in the first place anatase titania, zirconia, hafnia, and these in particular when partially modified with tungstenia (of higher altervalent capacity, six *versus* four), primarily impose and substantially feature the selective and specific membrane properties [24], with spillover of the primary oxide dipoles [13,14]:

$$Ti(OH)_4 + M \rightarrow Ti(OH)_3^+ + M\text{-}OH + e^- \quad (1a)$$

$$Ti(OH)_3^+ + 2\,H_2O \rightarrow Ti(OH)_4 + H_3O^+ \quad (1b)$$

$$M + 2H_2O \leftrightarrow M\text{-}OH + H_3O^+ + e^- \quad (1)$$

In fact, gels (aero and xerogels) are biphasic systems in which water molecules are trapped inside an oxide network, and such a material can be considered as a water-oxide membrane composite [24].

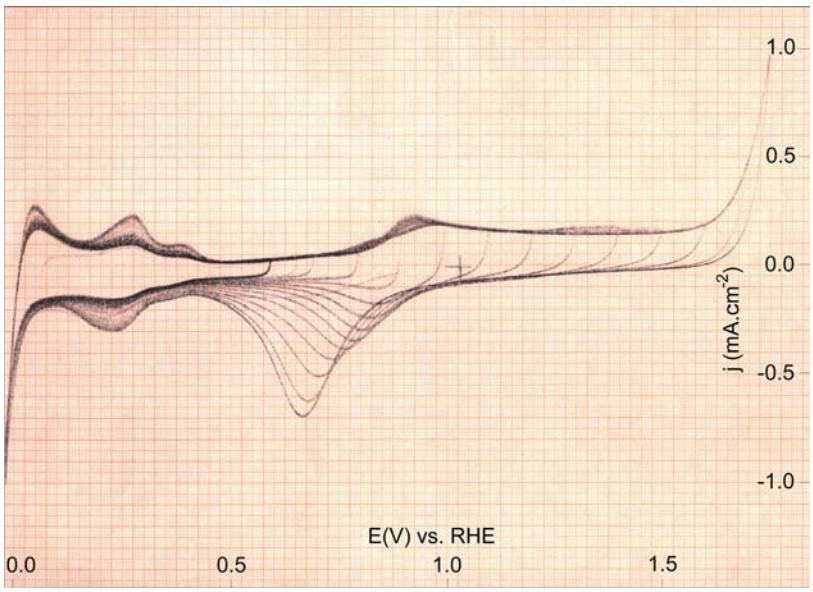

Fig. 6. Cyclic voltammograms of polycrystalline Pt (90 % in (111) crystal structure), stepwise scanned after a double layer charging range in 0.10 M NaOH at the sweep rate 100 mV s^{-1}. The short potential interval of the reversible peak existence for the primary oxide (Pt-OH) growth and desorption is clearly marked after horizontal scans within the double layer charging range.

Such membrane properties are the consequence of a strong first principle thermodynamic confirmation (density functional calculations, DFC) [25,26], that water molecules undergo spontaneous dissociative adsorption on anatase and even rutile titania surfaces. More specifically, the (101) surface of anatase characterizes the molecular adsorption with partial dissociation (less than 50 %), while on the (001) surface occurs spontaneous and prevailing dissociative chemisorption of water molecules [25,26]. In addition, it has recently been shown by first-principle(s) molecular-dynamic simulations the existence of a mechanism for thermodynamically favored spontaneous dissociation of water at low coverage of oxygen vacancies of the anatase (101) surface [27], and conesquently to the Magneli phases as substantially suboxide structure, with respect to molecular adsorption. In fact, this is the status of reversible open circuit dissociative adsorption of water molecules at the equilibrium state, as a spontaneous thermodynamic effect, while the presence of the metallic part of the catalyst, a directional electric field (or, electrode polari-

zation) further disturbs such an established equilibria and dynamically imposes a further continuous dissociation of water molecules, along with their facilitated inter-membrane transfer.

The stronger the d-d-bonding, the less strong the intermediate (M-H, M-CO, M-OH) adsorptive strength, and as a consequence, the easier arises the cleavage of the latter, and thence, the higher the overall rate of the electrocatalytic reaction. As the consequence of these hypo-d-oxides featuring such exchange membrane properties, the higher altervalent capacity, the more pronounced and the higher spillover effect arises. Since supported nano-clusters upon conductive oxide substrates effectively interact only around the two-phase circumference, the SMSI exponentially tends to the maximal catalytic activity when metallic deposit approaches nearly monoatomic network distribution. Such achievements have been approached with a homogeneous network of Pt upon Magneli phases particularly for the ORR (Fig. 7). The same hypo-hyper-d-intermetallic bonding affinity has at the same time been used for the selective grafting of individual and prevailing hyper-d-electronic catalysts upon such interactive d-oxide supports [11-13]. Meanwhile, there are still missing chemically enough stable intermetallic phases in the nanostructured state, such as $MoNi_3$, WFe_3, $MoCo_3$, $TiNi_3$, $ZrCo_3$, $HfFe_3$, to stand for and withstand the challenges of electrocatalysts for the anodic hydrogen oxidation (HOR) at least in alkaline LT PEMFC (Low Temperature PEM Fuel Cells), and oxygen evolution (OER) for water electrolysis in new membrane type electrolysis. Namely, such so-called Brewer intermetallic phases [6-9] feature rather high negative enthalpies of formation and, in principle, extra stable properties, while oxophilic hypo-d-electronic components, if not properly built within the lattice, exhibit sensitive behavior against water molecules, oxides and oxygen [28]. In such a context, new prospects afford nano-sized tungsten bronze and metalloenzyme electrocatalysts [29] in combination with proper hyper-d-electronic intermetallic components; these are the subject of further intense studies and considerations and consistent in opening a new room for synergistic nanostructured catalysts.

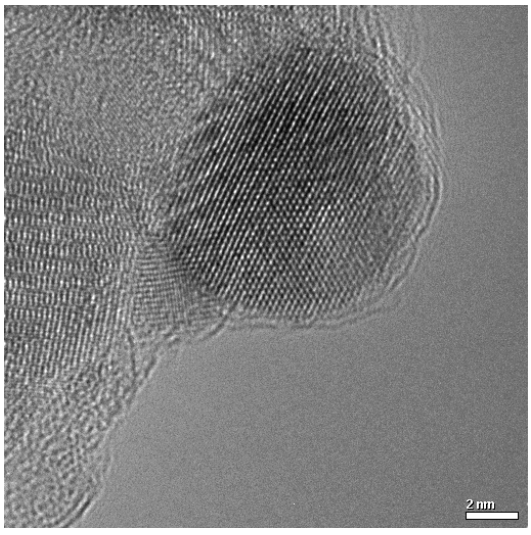

Fig. 7. HRTEM nanographs of nearly monoatomic network dispersion of Pt on Magneli phases (courtesy by M. V. Radmilović).

ADVANCED SPILLOVER KINETIC EFFECT OF PRIMARY OXIDES ON ELECTROCATALYSIS FOR THE ORR

The most outstanding electrocatalytic effect, substantially advanced by Magneli phases (trade name "Ebonex") [21] as the interactive support, has recently been substantiated by the extremely highly dispersed Pt sub-nanostructured of nearly monoatomic particle network (Fig. 7). Such Pt rather unusual deposit, as high as 36 $m^2 g^{-1}$ (monolayer Pt deposit has available surface of about 100 $m^2 g^{-1}$) upon a rather small (1.6 $m^2 g^{-1}$) available Magneli phase surface, was obtained from a 2-propanol solution of $Pt(NH_3)_2(NO_2)_2$ by the interactive grafting deposition followed by the reduction in a hydrogen stream at 300 °C [13,14]. The high resolution transition electron microscopy (HRTEM) analysis has shown Pt particle distribution between 0.1 and 1.0 nm, with prevailing monoatomic dispersion, though in average only every eighth Pt atom has been directly hypo-hyper-d-interelectronic bonded upon orderly distributed surface suboxide (oxygen vacant) Ti atoms of Magneli phases, the other having some sort of inter-platinum corrugated structure. Similar particle size in metal deposition so far has not been HRTEM recorded.

Polarization properties were exactly experimentally assessed on the basis of equivalent H-adatoms UPD estimated specific surface area and on the same exact basis compared with the most common market available Pt/Vulcan-XC-72 electrocatalyst (E-tek, Somerset, NJ, 10 wt. % Pt, 2-4 nm in size) for the ORR (Fig. 8) [13,14]. Kinetically controlled current density values at a potential of 0.85 V *versus* RHE, where the mass transfer effect is negligible, were 0.33 mA cm^{-2} for pure Pt/C and 0.61 mA cm^{-2} for Magneli phases--supported Pt (5.4 μg cm^{-2}, UPD of H-adatoms estimated, too), or twice different from each other in the order of magnitude.

The controversial point so far has been that the majority of papers dealing with the ORR consider the

transfer of the first of four electrons in the overall reaction of cathodic oxygen reduction for the RDS [29-34]:

$$O_2 + M + H_3O^+ + e^- \rightarrow M\text{-}OOH + H_2O \quad (2a)$$

$$M\text{-}OOH + M \rightarrow M\text{-}OH + M{=}O \quad (2b)$$

$$M\text{-}OH + M{=}O + 3H_3O^+ + 3e^- \rightarrow 5H_2O + 2M \quad (2c)$$

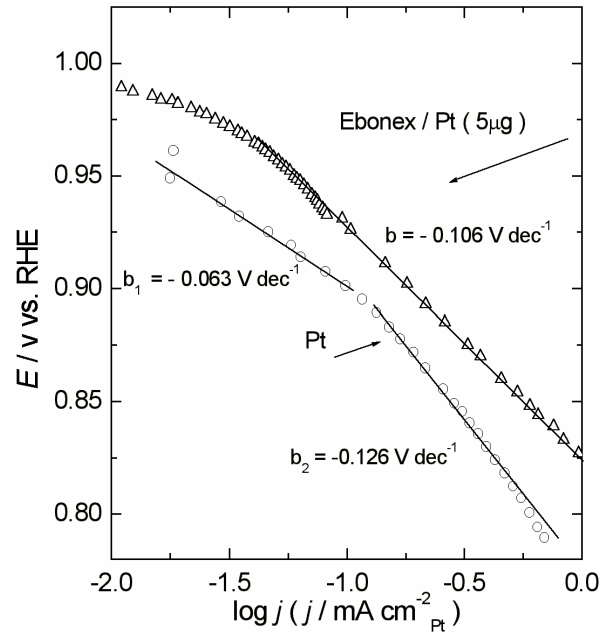

Fig. 8. Tafel plots for the cathodic ORR scanned on monoatomic dispersed and UPD estimated surface area (by desorption of H-adatoms) Pt network (5.4 μm cm^{-2}) upon Magneli phases (triangles) and nanostructured Pt (10 wt. % Pt on Vulcan XC-72, open circuits) in 0.50 M $HClO_4$ solution (backwards direction scan) [64,65].

but in controversy, the adsorbed primary oxide (Pt-OH) was considered to be the main obstacle and the rate determining (species) factor [35-40], regardless the broadly accepted fact that the latter participates in other fast steps of the overall mechanistic scheme (Eqs. (2a) and (2c)) [29,41,42]. However, the reversible reaction of the primary oxide formation and its reversal reduction (Eq. (1)) is extremely fast, and at the reduction potentials for ORR proceeds quite independently in both directions and undisturbed along with the H-adatom anodic oxidation in LT PEM FC. The point is that the reversible reaction of the anodic primary oxide formation and its cathodic reduction upon hypo-d-oxide supports, under wet conditions of a continuous moisture supply or a direct water contact, represents an unlimited source of the former (important for CO tolerance), but not so for the latter in the reverse direction. In fact, the whole membrane transferring mechanism (Eqs. (1a) and (1b)) features the redox properties and the higher the altervalent capacity, the higher the overall primary oxide effect. Thus, the present theory shows and experimental evidence testifies that cathodic ORR implies the continuous source of the primary oxide to be catalytically promoted. Such a continuous "pumping" effect for the primary oxide effusion or the spillover upon heterogeneous catalysts continuously feature the SMSI hypo-d-oxide catalytic supports, as long as the moisture supply in a gas phase is provided, or when the direct water contact exists in aqueous media electrocatalysis.

In the same context, in order to check the value of the coverage with oxygen containing species within the characteristic range of the potential close to the open circuit value and along the reversible part of the Tafel lines, for both Pt/Ebonex and polycrystalline Pt electrode nanostructured carbon-supported, some specific additional potentiodynamic measurements were carried out. The electrode, previously held at 0.20 V (RHE), was then shortly potentiostated at these just indicated and properly selected initial potential values within the low Tafel lines slope (Fig. 8), and afterwards the potential was linearly scanned from such characteristic initial values with the rather high sweep rate of 5.0 V s^{-1}, down to 0.0 V (RHE) (Figs. 9a and 9b, insets). Such a rather fast scanning rate in cyclic voltammetry is only applied when peaks of slow reaction steps should be avoided and/or for some reasons masked. The amount of charge imposed during such scans, determined by integration of *I-E* curves, proved that the surface coverage by oxide species on Pt/(Magneli phases) electrode was negligible and decreasing with successive negative potential values, the adsorption conditions being Langmuirian. These rather specific measurements even more clearly and convincingly show that the cathodic ORR upon Pt/Ebonex starts and finishes at remarkably and distinctly more positive potential values (1.05 down to 0.86 V, *versus* 0.95 down to 0.8 V, all taken *versus* the RHE), relative to polycrystalline Pt metal and/or Pt/C. In other words, within the reversible range of low Tafel line slope, the ORR proceeds upon the oxide covered Pt surface, as at its open circuit potential, while the plain Pt surface, deprived from its oxides, requires much higher polarization for the same reaction to occur. Such an experimental discovery and the approved evidence are of deeper fundamental significance. In such a respect, the interactive hypo-d-oxide supported Pt electrocatalyst apparently has the remarkable advantages for the overall reaction mechanism in the ORR, including its effusion or the spillover effect of the primary oxide (Pt-OH).

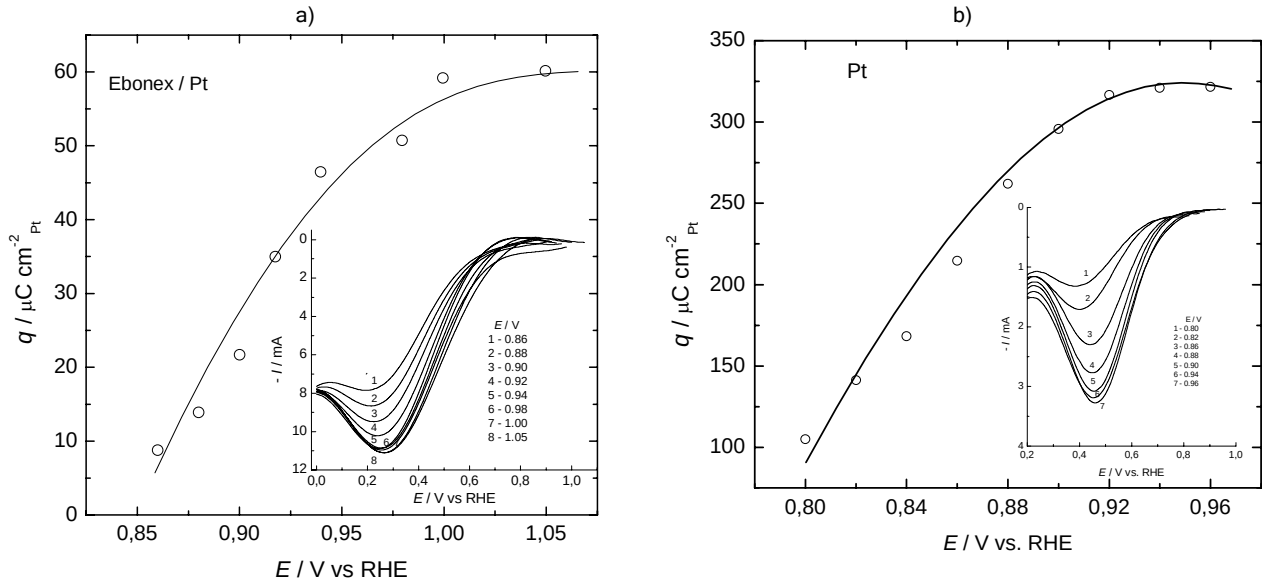

Fig. 9. a) Charge density that required oxygen species for their reduction, presented as a function of potential for Pt/Magneli phases (5 μg) electrode, same as in Fig. 8. The insert shows potentiodynamic I vs. E relations scanned from different initial potentials (hold) with sweep rate of 5.0 V s^{-1}. Where are Pt-OH species to impose the RDS?; b) the same as a), but for polycrystalline Pt metal. (Notice the ordinate scales.

Nonfaradaic promotion (NEMCA) [43-45] of hydrogen oxidation on Pt in water solutions does not impose any facilitating effect in acidic media [46], that reveals the retarding influence of hydronium ions at the low pH values, but there is no negative anionic influence and the role of hydroxide ions has been inferred to be decisive and NEMCA pronounced even in the plentiful of mineral ionic presence.

SOME UNIQUE SPECIFIC PROPERTIES OF THE PRIMARY OXIDE

The reversible fast reacting primary oxide (M-OH) arises monolayer adsorbed and distinctly marked by the charge capacity of a specific potentiodynamic peak, as the first step of water oxidation (Eq. (1)), immediately after the double layer charging range of many metals (Fig. 6). Due to its chemically rather unstable reactive features, and consequently so rather fast decomposition, leading to the irreversible and stable surface oxide (M=O) formation, the corresponding reversible peak extends within a rather narrow potential range. Similar behavior feature some other transition metal oxides of common formulas and structure, like MoO(OH), NiOOH, WO_2(OH) and can be identified both by the corresponding peaks within their potentiodynamic and XP spectra [13-15]. The point is that all transition metals of any, or in particular high altervalent capacity, afford the reversible primary oxide type states, usually of pronounced catalytic activity and even rather high electronic conductive properties (WO(OH), MoO_2(OH), Pt-OH, Au-OH), but unfortunately, in their oxidation sequences end-up with non-conductive and catalytically inactive higher valence oxide states (MoO_3, WO_3, Pt=O, Au=O, NiO_2), otherwise the whole aqueous electrochemistry would feature another and quite different physiognomy.

The primary oxide species behave dipole properties with prevailing ionic character of the majority of charge being transferred to the metal catalyst (Scheme I), and thus appear weakly adsorbed at the interface [47,48]. Such a state of the adsorptive binding strength varies from the less towards catalytically more active individual transition metals, or from the lower towards the higher d-band electronic filling (density), or from the stronger to the weaker adsorptive bonds decisive for the rate determining step (RDS), and substantially defines the overall electrocatalytic activity for both the HER and ORR. This is the core of the substantial difference between the reversible and fast reacting primary oxide relative to the highly polarizable surface oxide, whose polarization difference amounts for more than 600 mV (Fig. 6). Meanwhile, this is the reason of the potential axis coincidence that reversibly adsorbed both H-adatoms and primary oxides feature almost the same enthalpies of the adsorptive bonding upon catalytically active transition metal electrode substrates [47].

Although their existence arises clearly indicated by XP and potentiodynamic spectra [13-15], the primary oxides feature some unique specific fluent (jellium [49], or fluid) structure of dipoles with noticeable

Pauli repulsion (the spillover precondition) between adjacent M-OH species (Scheme I). The latter causes their rearrangement into an anti-parallel structure (OH-adsorbate being oriented in the upright position, with the O-atoms closest to the metal plane [47]), and consequently, there is no surface change monitoring in the course of the *in situ* STM scans [48], as might be expected and should be imposed and associated along with the corresponding charge transfer for their adsorptive generation within the reversible potentiodynamic peak [50,51]. The M-OH adsorbates are attracted towards and prefer the high coordination three-fold hollow sites on all transition elements, the adsorption energy for hollow and on-top sits being comparable for all d-metals, and consequently, they donate some electric charge to the surface to establish a dipole state (Scheme I), in particular when in addition, a positive polarization field is imposed. The trends in the bonding of the primary oxide has been similar in its nature to the surface oxide (M=O), with a substantial distinction that the weaker covalent interaction with the d-states is due the lower degeneracy of the OH*-species 1π level in comparison with 2p level of M=O, and in addition, the presence of the hydrogen atom, which pools the whole OH-species away from the surface (as confirmed by dipole moment measurements) [47]. Such typical dipole repulsive features stay in the core of the spillover properties of primary oxides. On the contrary, the H-adatoms form an essentially covalent adsorptive bond with transition metals, and thereby, the effect of the exerted electric field upon them is of much smaller impact. The Pauli repulsion becomes predominant due to the increased electron density on the primary oxide adsorptive state with an open-shell electronic configuration. The difference in adsorptive bonding upon different d-metals is primarily explained by diversities in interaction with the d-band states, since transition metals are characterized by a broad sp-band and a much narrower d-band, the latter being both the cohesive and adsorptive orbital, but with much higher density of electronic states. Due to the interactive nature for adsorbing species, the main bonding interaction of which is covalent, the binding energies at the metal/vacuum and metal/liquid interfaces are comparable, whereas the H-adatoms and M-OH adsorption energies do not exert any significant field dependence [47]. In fact, the main reason why electrode reactions involving various adsorbed hydroxo-species are potential dependent is because the electrons are taken from or stored at a different Fermi levels [52], and consequently, for transition metals the adsorptive bond becomes stronger with a lower d-band filling [47].

EXPERIMENTAL EVIDENCE FOR THE SMSI d-d-EFFECT

For the Au/TiO_2 interaction, rough and high surface area nanocrystalline anatase titania thin films were prepared on microscopy glass slides applying the doctor-blade procedure [53,54]. Rather fine and thin Au films were deposited by the electron beam evaporation of an Au wire of ultrahigh purity under vacuum higher than 6×10^{-4} Pa, onto stationary, titania coated microscopical slides, placed in parallel to the emitting surface. Quartz crystal monitor was used for controlling the deposition rate of 0.01 μg cm^{-2} s^{-1}. To elucidate the gold valence state and Au/TiO_2 binding energy for different thiny Au deposits, X-ray photoelectron spectroscopy (XPS) experiments were carried out in an ultrahigh vacuum chamber equipped with a hemispherical electron analyzer (SPECS LH-10) and twin-anode X-ray source, using unmonochromatized Mg-K_α at 1253.6 eV and an analyzer pass energy of 97 eV.

The XP spectra of the Au 4f electrons reveal the remarkable binding shift (Fig. 10), that provides evidence for the d-d-SMSI on the interphase Au/TiO_2 and this is one of the first experimental records for this kind of the catalyst-hypo-d-oxide binding in heterogeneous catalysis. The smaller the nanoparticle size or the thiner the nano-layer of Au deposit, as theoretically predicted in the present paper, the larger arises the binding energy shift in XP spectra with titania, and, consequently, the more pronounced the d-d-SMSI effect, with a tendency to its maximal d-d-binding effectiveness at monoatomic dispersion and with 1:1 deposition of Au on available Ti atoms. Namely, the thinner the nano-layer, closer to the interphase (Au/TiO_2) spectral beams penetrate and thereby, better and more completely reflect the bonding status within the latter.

The deconvoluted Au 4f peaks with lower Au loadings reveal that Au nanoparticles in interactive bonding contact with titania appear partially oxidized [55,56]. The peak located at 82.15±0.1 eV is identified and attributed to metallic Au, while the peak at 84.05± ±0.1 eV is situated at higher binding energy by 1.9 eV and corresponds to the gold primary (Au-OH or AuOOH) oxides. The latter, in accordance with the present theory, appear as *a priori* provided primary oxide spillover species, associated with anatase titania interaction (Eq. (1)), and are in advance, already available for anodic CO oxidation.

Haruta *et al.* [57] have shown that the same reactants (propylene in admixture with equimolar amounts of hydrogen and oxygen) yield different products upon different nano-sized Au catalysts supported on anatase titania (Au/TiO_2): (i) propane by hydro-

genation at nano-particles < 2nm Au, and (ii) propylene oxide by epoxidation or oxygen addition for > 2nm Au. Hydrogenation implies H-adatom adsorption upon Au that never spontaneously occurs on a pure massive bulky gold surface. Haruta [58-63] ascribes such chemisorptive properties to "forced" or strained Au-d-orbitals, in particular when d-d-SMSI deposited on the interactive anatase titania. In other words, the rather smaller nanostructured Au particles interactively d-d-bonded upon anatase titania (Au/TiO_2), thereby being exposed with the strained d-orbitals, are qualitatively something else than massive Au, behave H-adatoms adsorption, thus provide the reversible behavior of hydrogen electrode in the Nernst sense [13,64], and thence, finally are able to carry out the hydrogenation processes.

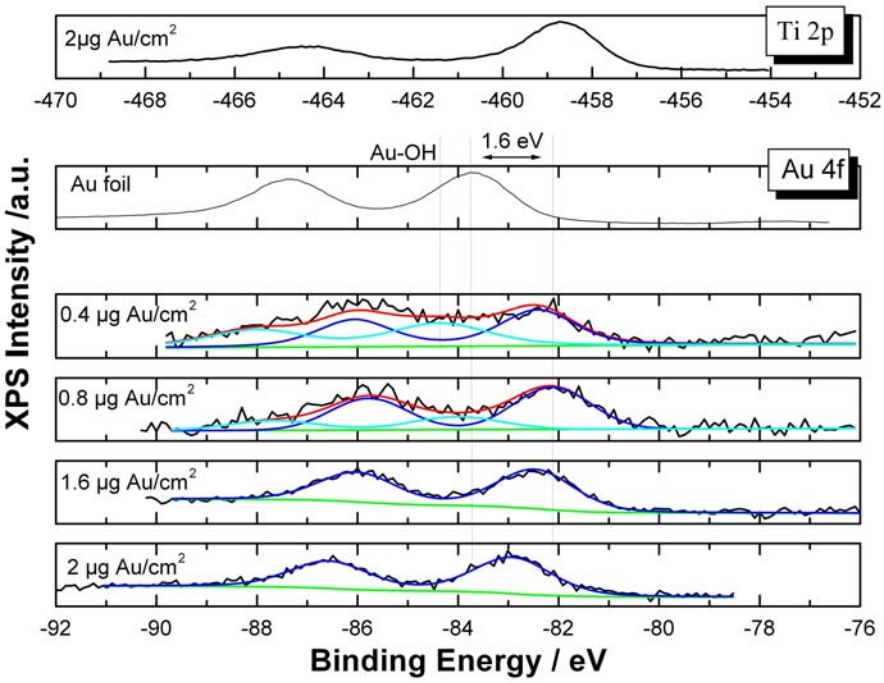

Fig. 10. XP spectra of Au 4f for vapor deposited nanostructured Au upon a fine thin film of anatase titania with deconvolution for lower amounts of deposits to reveal the existence of primary oxides (Au-OH and AuOOH) (courtesy by P. Falaras) [54].

XPS evidence for the primary oxide presence

In order to understand the origin of the oxidation states of Pt deposited on TiO_2, *ex situ XP* spectra of Pt $4f_{7/2}$ and O 1s photoelectrons are shown for the cases of 10 wt % $Pt/TiO_2/C$ before (Fig. 11a) and after the exposure in hydrogen stream at 573 K (Fig. 11b), followed by the continuous heating of the sample under UH-vacuum [13-15]. The binding energy of Pt 4f photoelectrons is located at 72.8 eV before the reduction in a hydrogen stream, and it is deconvoluted into two peaks with binding energies at 72.8 and 74.6 eV. After heating, there appears a major Pt 4f state at 71.34 eV, together with the state at 72.8 eV, and a smaller peak at 75.2 eV. The peak at 72.8 is attributed to Pt^{2+}, due to its combination with OH in the primary oxide (M-OH type), or eventually some other O species [66,67], while the peaks at 74.6 and 75.2 are attributed to the surface oxide, PtO_2 [68]. It would be worthwhile noting that, after heating, the corresponding O 1*s* XP spectra shows a pronounced decrease in the intensity of hydroxyl species (BE = = 532.2 eV) within anatase titania. Such a transformation stays in direct correlation with the reduction/transformation taking place at the same time and under the same conditions, as already observed with Pt species themselves (Fig. 10b). As a conclusion, such an experiment strongly indicates that oxidized Pt species, which are formed on the TiO_2 surface, due to the dissociative moisture effect of the latter [25-27], most probably originate from the spillover transfer of M-OH from the TiO_2 support onto the Pt crystallites [11-15,64].

The same type of XPS investigations with various composite $MoPt_x/TiO_2/C$ (x = 1 to 4) catalysts strongly indicate, besides the primary and surface Pt oxides, the prevailing presence of the primary oxides of Mo (MoO(OH) and $MoO_2(OH)$), otherwise being decisive for the spillover transfer in the anodic CO oxidation (*in situ* FTIR confirmed) [13,15].

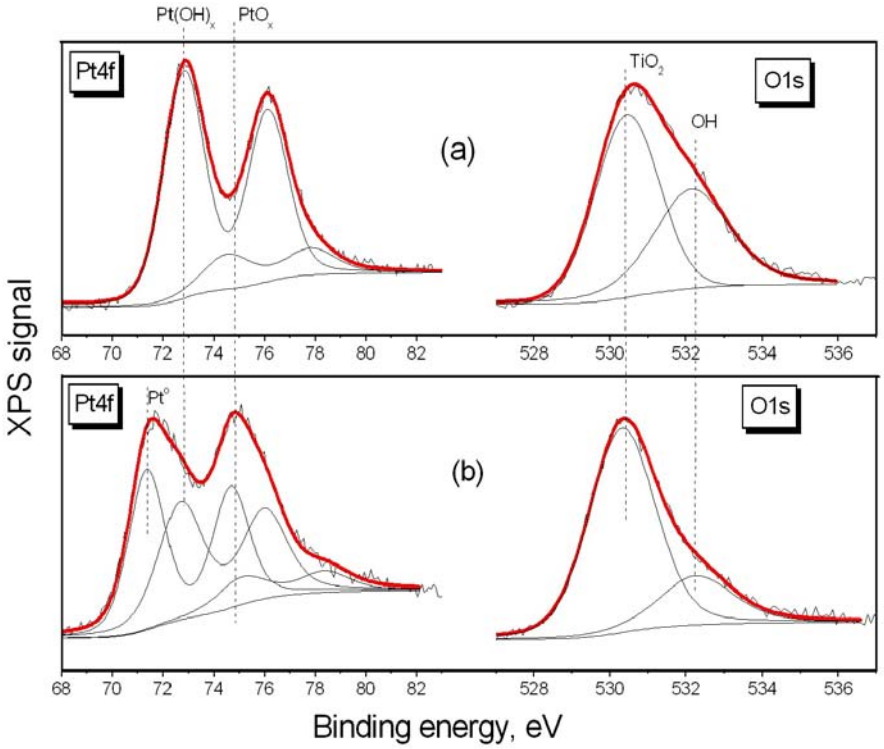

Fig. 11. Deconvoluted Pt 4f and O1s XP spectra of 10 wt. % Pt/TiO_2 catalysts before (a) and after the exposure/reduction in a hydrogen gas flow at 573K (b) [13,15].

Potentiodynamic evidence for the primary oxide spillover phenomenon

The spillover evidence by potentiodynamic scans in typical LT PEMFC arises as the most convincing confirmation. Potentiodynamic scans upon Pt/TiO_2/WO_3/C electrocatalyst deposited on Nafion 117 membrane repeatedly at low moisture content of He stream reveal a typical voltammograms characteristic of Pt metal itself, but with the reversible peaks of the primary oxide growth and the reduction taking place even within the usual double layer charging range. Meanwhile, a continuous supply of saturated water vapor in the He stream at higher temperature (80 °C), imposing condensation and leading to the appearance of rather wet titania-tungstenia mixed oxide (5.0 mol. % WO_3), as catalytic support, in particular with potential scans penetrating deeper within anodic range, are accompanied with an unusual phenomenon of a dramatic expansion of both reversible peaks of the primary oxide (Pt-OH) deposition and desorption in their charge capacity, both being shifted towards much more negative potentials (Fig. 12). Every ceasing in the steam supply immediately leads to the sudden reversible shrinkage of such rather exaggerated primary oxide peaks down to the initial typical shape of Pt voltammogram, and *vice versa*, renewed saturate water vapor feeding leads to their repeated sharp growth. Such an appearance behaves as a typical reversible phenomenon by its endless repetition, and never appears upon the plain Pt/C electrocatalyst. This dramatic and unusual phenomenon is doubtless associated with the spillover of primary oxide from the titania/tungstenia support and represents its best heuristic experimental confirmation, and nothing else. In fact, such a phenomenon is a unique and strong indication of the appearance and continuous proceeding of the primary oxide spillover, as long as the moisture supply proceeds along with the polarization (the "pumping water effect"). The latter results as the facilitated and well marked accompanying effect of the rather distinctly pronounced reversible charge capacity growth in both the anodic (adsorptive generation) and cathodic (desorptive) scan directions within potentiodynamic spectra. Since two different cyclic voltammogram shapes appear only as the result of the difference in water vapor supply, all other parameters being the same, just in accordance with the above theoretically displayed membrane type features of hypo-d-electronic oxide supports (Eqs. (1a) and (1b)), an unequivocal conclusion is imposed and defined as being derived from the interactive character for the primary oxide spillover transference. The creation of such a highly distinct Pt-OH spillover behavior, primarily based on the wetness and the spontaneous

adsorptive dissociative adsorption of water molecules [25-27], has its clearly announced a hint in Fig. 11.

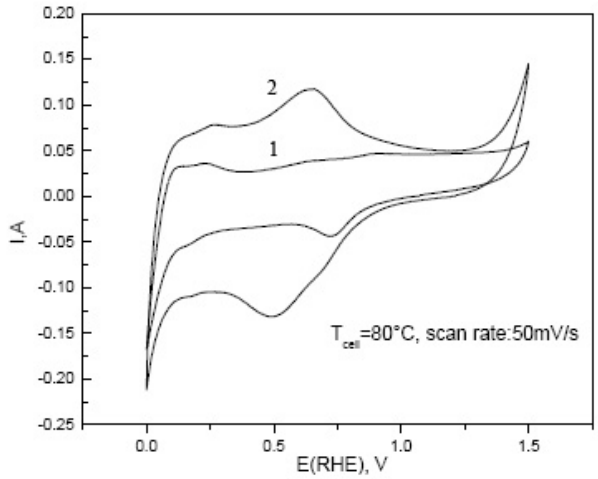

Fig. 12. Cyclic voltammograms of mixed hypo-d-oxides--supported nanostructured Pt electrode (Pt/TiO_2,WO_3), deposited upon DuPont Nafion 117 membrane and imbedded in a typical LT PEMFC, scanned in He stream, ones at low moisture content (curve 1) and at water vapor saturation (curve 2).

It should be inferred that mixed anatase (and even rutile) titania and tungstenia form intermolecular solid oxide solutions of a rather high altervalent capacity, compatible both in amorphous and crystalline forms of the corner sharing WO_6 and edge sharing TiO_6 octahedrons, with pronouncedly increased electrochromic features even at rather high contents of the latter [69,70]. In fact, highly charged W^{6+} cations favor the reversible acid dissociation of water molecules and thereby such electrochromic layers exhibit a well defined ion exchange and electron conductive properties [24].

Another potentiodynamic evidence of the primary oxide spillover is associated with anodic CO oxidation. Namely, ever since Watanabe and Motoo [71] have shown that Ru even in a submonolayer deposit, or while alloying with Pt, shifts the primary oxide growth to much more negative potential range and enables CO tolerance, the primary oxide spillover became of substantial significance for LT PEMFC. Similarly, the hypo-d-oxide supported Pt and Au (Pt/TiO_2, Au/TiO_2) in their behavior *versus* these two pure metals themselves, or their alloys, and/or RuPt and $RuPt/TiO_2$, are quite different couples of distinctly different catalytic properties, too, the SMSI issues featuring even a rather more pronounced primary oxide spillover effect. Since hypo-d-oxides, primarily anatase titania, zirconia and hafnia, facilitate spillover of M-OH, Fig. 13 clearly and accordingly shows the overall effect and the advantages of the membrane type OH^- – transferring within TiO_2 network of a catalyst support (SMSI), finally resulting in the primary oxide (M-OH) spillover, relative to the plain carbon. In other words, while Ru itself facilitates Pt-OH and Ru-OH spillover transfer in RuPt composite electrocatalyst [71], the supporting (SMSI) effect of titania, advances the whole same effect for more than 300 mV relative to RuPt/C catalyst (Fig. 13). Tseung [72,73] has already achieved a very similar result with macrostructured Pt-bronze (in fact, Pt wire surrounded by tungstenia, Pt/WO_3). Anodic CO oxidation starts even within the potential range of UPD desorption of H-adatoms (Fig. 13), and becomes much more pronounced in the charge capacity. This remarkable result is one of the most significant confirmations of the present interactive and dynamic spillover catalytic model, as implemented in electrocatalysis.

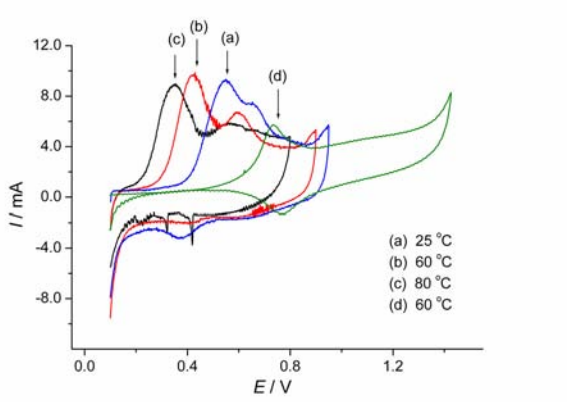

Fig. 13. The striping voltammograms for CO desorption from supported 10 wt. % (0.4 mg cm^{-2}, 2 nm in average size, 1:1 atomic ratio Ru:Pt) RuPt/TiO_2/C electrocatalyst CO-saturated at three different temperatures: 25 (a); 60 (b) and 80 (c) °C, scanned at the scan rate of 2 mV s^{-1}; (d) the same stripping scans for CO desorption at 60 °C from unsupported 30 wt. % (0.5 mg cm^{-2}, same average nano-size) E-tek RuPt/C electrocatalyst of the same RuPt nano-size, atomic ratio and load, and sweep rate 10 mV s^{-1} and its CO saturation at 55 °C.

In fact, plenty of potentiodynamic evidence upon non-supported Pt and Au electrodes testifies that whenever there exists enough supply of species of rather fast oxidation ability, being much faster than the next step of M-OH transfer into the stable surface growing oxide (Pt=O) layer, such as various aldehydes, saccharides and simple alcohols, their anodic oxidation starts at the characteristic aldehyde reversible potential close to UPD desorption of H-adatoms [74]:

$$R\text{-}CHO + M\text{-}OH + H_2O \rightarrow R\text{-}COOH + M + H_3O^+ + e^- \quad (2)$$

proceeds all along the double layer range, arises the concentration polarized and extends almost to the oxygen evolving limits (Figs. 14 and 15). In fact, if any aldehyde oxidation was based upon a direct electron exchange reaction, such a catalytic peak would be of distinctly shorter potential range. Since the surface oxide (Pt=O) growth becomes dramatically suppressed all along the anodic scan by the competitive and faster parallel aldehyde oxidation with the continuously generated primary oxide (Pt-OH), its cathodic desorption peak arises dramatically reduced in the charge capacity. After its removal, the anodic aldehyde oxidation peak again grows along the reverse cathodic scan direction, and arises much more pronounced at higher concentrations of the reacting species (Fig. 15). Such cyclic voltammograms are the best evidence of the reversible features for the primary oxide growth and reduction (Eq. (1)), and its thereby rather fast reaction rates, the latter being controlled by the concentration polarization. Such a reaction becomes in particular fast in contact with hypo-d--oxide supports, as the continuous source of the primary oxides and their pronounced spillover transfer by the interactive mechanisms of the SMSI (Eqs. (1a) and (1b)).

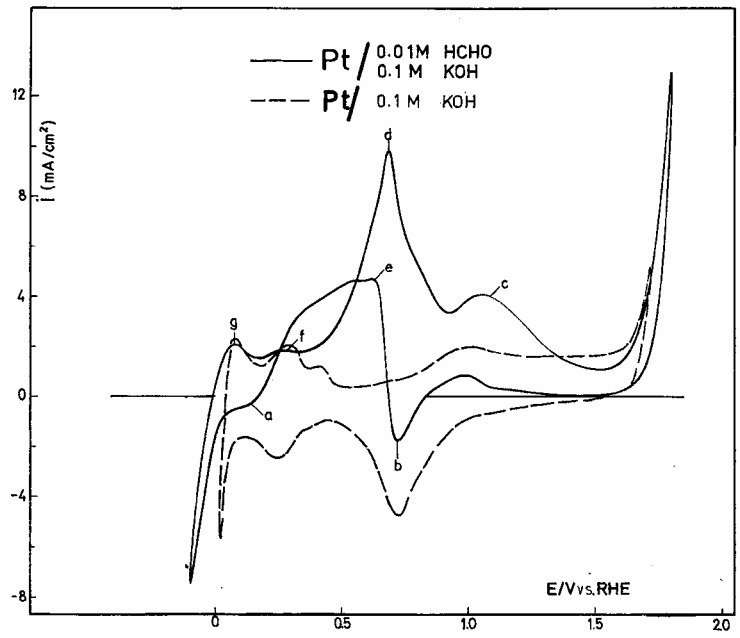

Fig. 14. Cyclic voltammograms scanned on a polycrystalline Pt wire electrode in alkaline (0.10 M KOH) solution in admixture of formaldehyde (0.010 M HCHO) at 200 mV s^{-1} sweep rate between hydrogen and oxygen potential evolving limits. Labels: a - reversible hydrogen adsorption peak; b - primary irrevrsible surface oxide (Pt=O) desorption peak; c and d - successive peaks of aldehyde oxidation; e - sudden sharp current jump and reverse peak of repeated aldehyde oxidation; f and g - reversible hydrogen oxidation and desorption peaks [74].

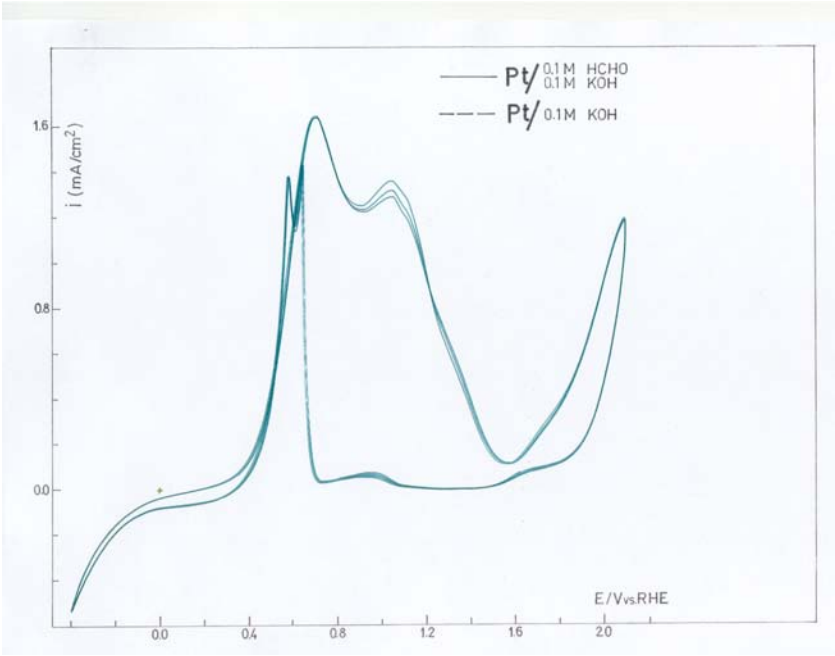

Fig. 15. The same as in Fig. 14, but with 0.10 M HCHO [74].

TOWARDS THE REVERSIBLE OXYGEN ELECTRODE

The discrepancy in electrocatalysis for the hydrogen fueled LT PEMFC is that the room for further advances in the activity for the ORR, relative to the HOR and HER, amounts for more than 400 mV and has motivated the search towards the reversible oxygen electrode for two centuries. A step ahead has been imposed when the fine nanostructured Pt catalyst was deposited on highly electron conductive and interactive Magneli phases [64,65], and thereby revealed the extension of the reversible range for the ORR along the Tafel plot (Fig. 8). Such state of the experimental evidence along with theoretical knowledge concerning the properties of the primary oxides and their role in heterogeneous catalysis and electrocatalysis, traces the pathway towards the (nearly) reversible oxygen electrode, primarily for LT PEMFC. This first of all relates the nanostructured tungsten (or the composite titania-tungstenia oxide supports) bronze and modified bronzes, so far never achieved in experimental practice nor applied in electrocatalysis. The experiments with a macro-sized wired Pt/WO_3 bronze [72,73], impose rather reliable expectancies in such a respect. In other words, such expectancies are based and relied on the composite and higher altervalent hypo-d-oxide support effect in the continuous supplying "pumping" properties of the primary oxides. For the same reasons, similar expectancies impose the nanostructured hyper-d-oxides electrocatalysts supported on the conductive and (SMSI) interactive altervalent oxides, such as RuO_2,IrO_2/WO_3. Such trends and expectancies to extend the reversible Tafel range of the interactive supported nano-sized electrocatalysts and create, at least the nearly reversible oxygen electrode, are the subject matter of the forthcoming papers of the present authors.

The main far-reaching conclusion of the present paper has been that electrocatalysis for hydrogen and oxygen electrode reactions are primarily the d-band defined, since the latter is the proved bonding, adsorptive and electrocatalytic orbital. In fact the state of the d-band, such as the d-electronic density of states, the position of the center of antibonding peak relative to the Fermi level or its strained status, are the actual and decisive catalytic operational parameters in search for the synergism in electrocatalysis, as the result of just displayed d-d-electronic correlations. In such a respect, the interactive supported hypo-hyper-d-d-interelectronic combinations afford the most promising electrocatalysts since the optimal average d-electronic configuration coincides with the strongest interelectronic bonding effectiveness and the most stable, often extra-stable intermetallic phases with prevailing hyper-d-electronic ingredient, while the SMSI further advances the overall catalytic effect.

Acknowledgements

The present work has been supported by the Ministry of Science, Technologies and Development, Republic of Serbia, under Contract No. 142038, and carried out within EU Project "*Prometheas*", Contract No. ICA2-2001-10037, too, and enters (in) the core of the proposed IP7 EU Project "STRONGCAT" in Nanoscience and Nanotechnology.

REFERENCES

[1] S. J. Tauster, S. C. Fung, J. Catalysis **55** (1978) 29
[2] S. J. Tauster, S. C. Fung, R. T. K. Baker, J. A. Horsley, Science **217** (1981) 1121
[3] S. A. Stevenson, *Metal-Support Interaction in Catalysis, Sintering and Redispersion*, Van Nostrand, New York, 1987
[4] G. L. Haller, D. E. Resasco, Adv. Catalysis **36** (1989) 173
[5] M. M. Jaksic, J. New Mat. Electrochem. Systems **3** (2000) 153
[6] L. Brewer, Science **161** (1968) 115
[7] L. Brewer, in*: Electronic Structure and Alloy Chemistry of Transition Elements*, P. A. Beck Ed., Interscience, New York, 1963, p. 221
[8] a) L. Brewer, in *High-Strength Materials*, V. F. Zackay, Ed., Wiley, New York, 1965, p. 12; b) L. Brewer, *The Cohesive Energies of the Elements*, LBL-3720, Berkeley, California, May 4, 1977
[9] L. Brewer, In *Phase Stability in Metals and Alloys*, P. Rudman, J. Stringer, R. I. Haffee, Eds., McGraw-Hill, New York, 1967, p. 39
[10] S. G. Neophytides, S. Zafeiratos, G. D. Papakonstantinou, J. M. Jaksic, F. E. Paloukis, M. M. Jaksic, Int. J. Hydrogen Energy **30** (2005) 131, 393
[11] M. M. Jaksic, Electrochim. Acta **45** (2000) 4085
[12] S. G. Neophytides, S. Zafeiratos, M. M. Jaksic, J. Electrochem. Soc. **150** (2003) E512
[13] J. M. Jaksic, Lj. Vracar, S. G. Neophytides, S. Zafeiratos, G. Papakonstantinou, N. V. Krstajic, M. M. Jaksic, Surf. Sci. **598** (2005) 156
[14] J. M. Jaksic, N. V. Krstajic, Lj. M. Vracar, S. G. Neophytides, D. Labou, P. Falaras, M. M. Jaksic, Electrochim. Acta **53** (2007) 349
[15] S. Zafeiratos, G. Papakonstantinou, M. M. Jaksic, S. G. Neophytides, J. Catalysis **232** (2005) 127
[16] C. Kittel, *Solid State Physics*, 6th Ed., Wiley, New York, 1986
[17] B. C. Allen, Trans. Met. Soc. A IME **227** (1963) 1175
[18] H. Kita, J. Electrochem. Soc. **113** (1966) 1095
[19] M. H. Miles, J. Electroanal.Chem. **60** (1975) 89
[20] M. Methfessel, D. Hennig, M. Scheffler, Phys. Rev. B **46** (1992) 4816
[21] A. Magneli, Acta Chem. Scandinavica **13** (1959) 5

[22] P. Sabatier, *La Catalyse en Chimie Organique,* Librairie Polytechnique, Paris, 1913
[23] P. Sabatier, Ber. Deutsch. Chem. Soc. **44** (1911) 2001
[24] J. Livage, M. Henry, C. Sanchez, Prog. Solid State Chem. **18** (1988) 259
[25] A. Vittadini, A. Selloni, F. P. Rotzinger, M. Gratzel, Phys. Rev. Lett. **81** (1998) 2954
[26] M. Lazzeri, A. Vittadini, A. Selloni, Phys. Rev. B **63** (2001) 155409
[27] A. Tilocca, A. Selloni, J. Chem. Phys. **119** (2003) 7445
[28] M. Mavrikakis, P. Stoltze, J. K. Norskov, Catal. Lett. **64** (2000) 101
[29] Yuguang Ma, P. B. Balbuena, Chem. Phys. Lett. **440** (2007) 130
[30] A. Damjanovic, D. B. Sepa, M. V. Vojnovic, Electrochim. Acta **24** (1979) 887
[31] A. Damjanovic, A. Dey, J. O'M. Bockris, Electrochim. Acta **11** (1966) 791
[32] D. B. Sepa, M. Vojnovic, A.Damjanovic, Electrochim. Acta **26** (1981) 781
[33] D. B. Sepa, M. V. Vojnovic, Lj. Vracar, A. Damjanovic, Electrochim. Acta **31** (1986) 91
[34] a) J. O'M. Bockris, R. Abdu, J. Electroanal. Chem. **448** (1998) 189; b) J. O'M. Bockris, A. Damjanovic, J. McHardy, C.R. Troisieme Journ. Internat. d'Etude des Piles a Combustible, Presses Academique Europeenne, Bruxelles, 1969, pp. 15-28
[35] R. A. Sadik, A. B. Anderson, J. Electroanal. Chem. **528** (2002) 69
[36] S. Goetesfeld, T. A. Zawodzinski, in *Advances in Electrochemical Science and Engineering*, Vol 5, R. C. Alkire, D. M. Kolb, Eds., Wiley-WXH, Weinheim, 1997, pp. 197-297
[37] A. Anderson, Electrochim. Acta **47** (2002) 3759
[38] a) R. R. Adzic, in *Frontiers in Electrochemistry,* Vol. 5, *Electrocatalysis*, J. Lipkowski, P. N. Ross, Eds., VCH Publishers, New York, 1998, p. 197; b) N. A. Anastasijevic, V. B.Vesovic, R. R. Adzic, J. Electroanal. Chem. **229** (1987) 317
[39] S. Mukerjee, S. Srinivasan, in *Handbook of Fuel Cells,* Vol. 2, W. Vielstich, A. Lamm, H. Gasteiger, Eds., Wiley, Chichester, U.K., 2003, pp 502-519
[40] M. R. Tarasevich, Sadkowski, E. Yeager, in *Comprehensive Treatise of Electrochemistry,* B. E. Conway, J. O'M. Bockris, E. Yeager, S. U. M. Kahn, R. E. White, Eds., Plenum Press, New York, 1983, p. 301
[41] Y. Wang, P. B. Balbuena, J. Phys. Chem. B **108** (2004) 4376
[42] Y. Wang, P. B. Balbuena, J. Phys. Chem. B **109** (2005) 14896
[43] S. G. Neophytides, D. Tsiplakides, P. Stonehart, M. Jaksic, C. G. Vayenas, J. Phys. Chem. **100** (1996) 14803
[44] D. Tsiplakides, S. G. Neophytides, O. Enea, M. Jaksic, C. G. Vayenas, J. Electrochem. Soc. 144 (1997) 2072
[45] C. G. Vayenas, M. M. Jaksic, S. I. Bebelis and S. G. Neophytides, in *Modern Aspects of Electrochemistry*, Vol. 29, J. O'M. Bockris, B. E. Conway, R. E. White, Eds., Plenum Press, New York, 1996, pp. 57-202
[46] D. Labou, S. G. Neophytides, Topics in Catalysis **34** (2006) 451
[47] M. T. M. Koper, R. A. van Santen, J. Electroanal. Chem. **472** (1999) 126
[48] C. A. Vitus, A. J. Davenport, J. Electrochem. Soc. **141** (1994) 1291
[49] N. D. Lang, Comments Condens. Matter. Phys. **14** (1989) 253
[50] H. Angerstein-Kozlowska, B. E. Conway, A. Hamelin, L. Stoicoviciu, Elecctrochim. Acta **31** (1986) 1051
[51] H. Angerstein-Kozlowska, B. E. Conway, A. Hamelin, L. Stoicoviciu, J. Electroanal. Chem. **228** (1987) 429
[52] B. Hammer, J. K. Norskov, Adv. Catalysis **45** (2000) 71
[53] I. M. Arabatzis, S. Antonaraki, T. Stergiopoulos, A.Hiskia, E. Papaconstantinou, M. C. Bernard, P. Falaras, J. Photochem. Photobiol. A **149** (2002) 237
[54] I. M. Arabatzis, T. Stergiopoulos, D. Andreeva, S. Kitova, S. G. Neophytides, P. Falaras, J. Catalysis **220** (2003) 127
[55] M. Peuckert, F. P. Coenen, H. P. Bonzel, Electrochim. Acta **29** (1984) 1305
[56] J. E. Drawdy, G. B. Hoflund, S. D. Gardner, E. Yongvadotir, D. R. Schtyrer, Surf. Interface Anal. **16** (1990) 369
[57] T. Akita, K. Tanaka, S. Tsubota, M. Haruta, J. Electron Microscopy **49** (2000) 657
[58] M. Haruta, M., Catal. Today **36** (1997) 153
[59] M. Date, M. Haruta, J. Catalysis **201** (2001) 221
[60] F. Boccuzzi, A. Chiorino, S. Tsubota, M. Haruta, J. Catalysis **202** (2001) 256
[61] F. Boccuzzi, A. Chiorino, M. Manzoli, P. Lu, T. Akita, S. Ichikawa, M. Haruta, J. Catalysis **202** (2001) 256
[62] T. Akita, P. Lu, S. Ichikawa, K. Tanaka, M. Haruta, Surf. Interface Anal. **31** (2001).
[63] M. Haruta, The Chemical Record **3** (2003) 75
[64] S. G. Neophytides, K. Murse, S. Zafeiratos, G. Papakonstantinou, J. M. Jaksic, F. E. Paloukas, M. M. Jaksic, J. Phys. Chem. B **110** (2006) 3030
[65] Lj. M. Vracar, N. V. Krstajic, V. R. Radmilovic, M. M. Jaksic, J. Electroanal. Chem. **587** (2006) 99
[66] M. Peuckert, F. P. Coenen, H. P. Bonzel, Electrochim. Acta **29** (1984) 1305
[67] J. E. Drawdy, G. B. Hoflund, S. D. Gardner, E. Yongvadotir, D. R. Schtyrer, Interface Anal. **16** (1990) 369
[68] J. P. Contaur, G. Mouvier, M. Hoogewijs, J. Catalysis **48** (1997) 217
[69] S. Hashimoto, H. Matsuoka, J. Electrochem. Soc. **138** (1991) 2403
[70] S. Hashimoto, H. Matsuoka, Surf. Interface Anal. **19** (1992) 464
[71] M. Watanabe, S. Motoo, J. Electroanal. Chem. **60** (1975) 267
[72] A. C. C. Tseung, K. Y. Chen, Catalysis Today **38** (1997) 439
[73] A. C. C. Tseung, P. K. Shen, K. Y. Chen, J. Power Sources **61** (1996) 223
[74] N. M. Ristic, M. Kotorcevic, C. M. Lacnjevac, A. M. Jokic, M. M. Jaksic, Electrochim. Acta **45** (2000) 2973.

DR JELENA M. JAKŠIĆ

Jelena M. Jakšić graduated from the Faculty of Physical Chemistry, Faculties of Sciences, University of Belgrade in 1995, with two academic years of studies at the Departments of Physics and Chemical Engineering, University of Patras in Greece. Diploma thesis done with Professor Slavko Mentus on Non-Faradaic Electrochemical Modification of Catalytic Activity (NEMCA) for Heterogeneous Reaction of Hydrogen Oxidation in Aqueous Media was awarded by "the Belgrade October city prize" for creative contribution of youth on 20th October 1997. M.S. studies at the Center for Multidisciplinary Studies, University of Belgrade, Surface State Division, were completed in 2000 with Professors Nedeljko V. Krstajić, Milan Vojnović and Nikola Ristić on Kinetics of Hydrogen Evolution on Intermetallic Phases and Alloys of Ni, Co and Mo. Ph.D. degree was earned in 2004 from Faculty of Technology and Metallurgy, University of Belgrade with partial fulfillment at University of Patras, Greece in the frame of two EU research projects, "Prometheas" and "Apollon", on Kinetics of Electrochemical Hydrogen Evolution and Oxidation Reactions on Mo-Pt Alloys carried out with Professor Nedeljko V. Krstajić. Jelena received a one-year Greek Ministry of Science grant for her work on doctoral thesis. So far along with her supervisors Dr. J. Jaksic published 20 scientific papers in recognized international journals. Scientific interest includes electrocatalysis for hydrogen and oxygen electrode reactions and sophisticated surface characterization of catalysts.

PROFESSOR ČASLAV M. LAČNJEVAC

Associate professor at the Institute for food technology and biochemistry, Faculty of Agriculture, University of Belgrade. Born (1952) in Aleksandrovac, Kruševac, Serbia.
B.Sc. degree (1976) at the Faculty of Technology and Metallurgy, M.Sc. (1979) at the Center for Multidisciplinary Studies, and Ph.D. (1994) at the Faculty of Technology and Metallurgy, University of Belgrade.
Subject of interest: Kinetics and mechanism of electrode reactions (deposition of metals, hydrogen and oxygen evolution reactions), new electrode materiels, corrosion, corrosion protection, electro-organic synthesis.

PROFESSOR NEDELJKO V. KRSTAJIĆ

Professor at the Department of Physical Chemistry and Electrochemistry at the Faculty of Technology and Metallurgy, University of Belgrade. Born (1952) in Belgrade, Serbia.
B.Sc. (1978), M.Sc. degree (1981) and Ph.D. (1989) at the Faculty of Technology and Metallurgy, University of Belgrade. Post-doctoral research Fellow during 1992-1993 at the Department of Physical Chemistry and Electrochemistry, University of Milan, Milan, Italy.
Subject of interest: Kinetics and mechanism of electrode reactions (deposition/dissolution of metals, hydrogen, oxygen and chlorine evolution reactions), new electrode materiels (activated titanium anodes, electroconducting polymers, metal-hydride electrodes) corrosion, corrosion protection, electro-organic synthesis, electrochemical power sources.

PROFESSOR MILAN M. JAKŠIĆ

Professor Milan M. Jakšić graduated at Faculty of Technology, University of Belgrade in physical chemistry and electrochemistry with Academician Panta S. Tutundžić (1958). Industrial experience: Factory of Plastics and Chemical Products 'Jugovinil' at Kaštel Sućurac near Split, Manager of the electrochemical plant for chlorine and chlorate production, Department of Electrochemistry, Institute of Chemistry, Technology and Metallurgy in Belgrade, the principal investigator, founded Laboratory for industrial electrochemistry. Ph.D. degree with Academician Aleksandar R. Despić at Department of Physical Chemistry and Electrochemistry, Faculty of Technology and Metallurgy, University of Belgrade, in 1970, in "Advances in Modified Technological Process for Electrochemical Chlorate Production". Awarded by the traditional October price of Belgrade city for achievements and contributions in physical, mathematical and technical sciences within the jubilee of 1974 year celebrating thirty years of deliberation of Yugoslav capital city in the World war second. University career: Faculty of Technology at Split, University of Zagreb (later being University of Split), Lecturer in Electrochemical Processes and Electrode Kinetics (1963), Assistant Professor (1970). Department of Physical Chemistry, Faculties of Sciences, University of Belgrade, promoted for Associate Professor in Physical Chemistry of Surfaces (Surface State) at Center for Multidisciplinary Studies, University of Belgrade, group Surface State; the same status confirmed in Physical Chemistry (general course) in 1978 at Institute of Food Technology, Faculty of Agriculture; in 1984 advanced for Professor. Postdoctoral fellowship in electrochemical engineering (1976/78), as Fulbright-Huys grantee with distinguished Professor Charles W. Tobias at Department of Chemical Engineering and Lawrence Berkeley Laboratory (LBL), University of California at Berkeley, and again in 1984 as Visiting Professor with Professor John Newman. Visiting Professor with Professor Reidar Tunold at University of Trondheim, NTNU, Laboratory of Applied Electrochemistry (1989/90). Department of Chemical Engineering, University of Patras in Greece as Visiting Professor with Professor Costas G. Vayenas, invited to confirm Non-Faradaic promotion of heterogeneous catalytic processes (NEMCA) in aqueous media (1992/94). At University of Patras again as Visiting Professor Emeritus first again with C.G. Vayenas (2000), and further with Dr. Stelios G. Neophytides, Institute of Chemical Engineering and High Temperature Chemical Processes, FORTH and Professor Iannis Kallitsis, Department of Chemistry, University of Patras, work on EU projects in electroca-

talysis for Low Temperature PEM Fuel Cells and water electrolysis in membrane cells (2000-2005). Honored by the "Sir William Grove Award" of International Association for Hydrogen Energy for his “outstanding contributions to the theory of electrocatalysis of hydrogen electrode reactions”; awarded by Annual price of Union of University Professors of Serbia (1999). Since 1983, as one of three members Program Committee, along with distinguished Professors Sergio Trasatti, University of Milan, Italy, and Hartmut Wendt, Technische Hochschule, Darmstadt, Germany, organized five International Conferences on Electrocatalysis, (5th ECS’06, Kotor, 2006) with the highest excellence estimation by EU "Marie Curie Program". Published more than 120 scientific papers in distinct international journals, presented 74 plenary and keynote lectures and along with his coworkers about 400 papers at international and domestic scientific meetings, while about 100 seminars communicated at numerous universities worldwide (SCI above 1,300). Member of International Advisory Board of IAHE (International Association for Hydrogen Energy). Co-Editor of Belgrade International journal “Chemical Industry and Chemical Engineering Quarterly (CI&CEQ). Active member of Yugoslav Engineering Academy (now Academy of Engineering Sciences of Serbia) from 2001. Awarded for the first honorary citizen of his native Alaksandovac town (2004).